Modeling a Water Flow on an Icing Surface

P. Fu, M. Farzaneh*, G. Bouchard
NSERC/Hydro-Quebec/UQAC Industrial Chair on Atmospheric Icing of Power Network Equipment (CIGELE) and Canada Research Chair on Atmospheric Icing Engineering of Power Networks (INGIVRE) at the University of Quebec at Chicoutimi, Chicoutimi, Quebec, Canada,
http://www.cigele.ca

***Abstract*—Under wet-icing conditions, a thin water film forms on the icing surface. In order to estimate the thickness of the water film, which is needed for further analysis, it is necessary to model the motion of water flow on this surface. In this paper, a description of such a model will be provided, which will be used in the subsequent thermodynamic analysis. Next, the calculation method will be utilized to investigate a number of cases representing typical atmospheric icing conditions, where parameters such as the water-film thickness, water temperature and corresponding icing fractions will be relevant. Finally, the impacts of the new procedure on ice-accretion modeling will be discussed.**

1. Introduction

UNDER icing conditions, the icing surface is exposed to air-borne supercooled droplet impingements. Of the surface water collected from these impingements, one portion will instantaneously freeze at impact while the unfrozen potion will move over the surface under the combined action of gravity and air drag. Water flow was not usually accounted for in earlier model studies [17,21] because the unfrozen portion was assumed to shift completely to the adjacent surface element at each simulation step and thus rendering water film analysis unnecessary. Moreover in these studies, the surface temperature of the wet regime was assumed to be the freezing point of the water, and as a result, the thermal balance equation proposed by Messenger [22] may easily be applied for wet-icing regime.

Recently, a number of researchers [3,14,24,26] have studied the behavior of the icing surface water film. Bourgault et al. [3] modeled the surface water flow based on a shallow-water icing model, where the air shear stress τ is supposed to be the main driving force for the water film, which is particularly true in the case of the aircraft icing. A simplifying assumption in his model consists in supposing the velocity to be linear in the n direction, normal to the surface. In Karev' study [14] on the thermodynamic behavior of a wind-sheared supercooled liquid film flowing on a plate, the mean water-film velocity is estimated according to the Couette linear profile, and is thus a function of the water-film thickness. Also in this paper, the impact of the water film on icing thermodynamics is assessed. However, it is impossible to calculate the thickness of a water film unless the solution to momentum differential equations coupled with the equation of conservation of mass for the surface water flow is achieved.

Myers [24] proposed a mathematical model to simulate the momentum behavior of the water film. His main contribution lies in the fact that the momentum water flow model is linked to a Stefan model which is specifically used to govern the phase change at the water-ice interface. His model consists of a number of Navier-Stokes and continuity equations which are eventually coupled with other relevant calculation components of the aircraft icing model [8]. Theoretically, his algorithm ensures continuity and physically sensible results for the water height as well as mass conservation. However, seeking a converging solution to these coupled differential equations is not an easy task.

The present paper proposes a new method for modeling the water flow on an icing surface. In this method, the water film is considered to be a steady flow on a flat plate [5]. The water film tends to move over the icing surface under the action of external forces, one part of the water film moving upwards while the remainder running downwards. It is not necessary for the runback water to start its motion at the stagnation point, as has been assumed by a number of researchers. The starting point is defined as the location at which the effects of the external forces cancel each other out, and where the water-flow undergoes a change in direction. Once the flow direction on any particular surface element is known, it is possible to establish the calculation sequence and determine the amount of water gained from the preceding element together with the amount discharged to the next one.

2. Model Descriptions

This study was carried out using the icing model developed at CIGELE [6], which consists of a number of calculation components. Of these components in the model, the role of airflow computation is pivotal, since the output of this calculation provides the basic parameters for subsequent components. In particular, airflow field is solved by using the boundary layer theory, in which the fluid field under study is viewed as a potential flow combined with boundary layer. The potential flow region is considered to be the superposition of a uniform flow and a disturbance flow which may be solved using the Boundary Element Method (BEM). The fluid boundary layer is evaluated in terms of the velocity distribution on the common boundary as obtained from the preceding potential flow calculation. The Runge-Kutta numerical algorithm is used to solve the differential equations of motion, so as to obtain droplet trajectories, thereby

*CIGELE/INGIVRE Chairholder

evaluating the local impingement efficiency [26]. Figure 1 shows the airflow velocity field and trajectories of water droplets in the vicinity of an icing object using the icing model.

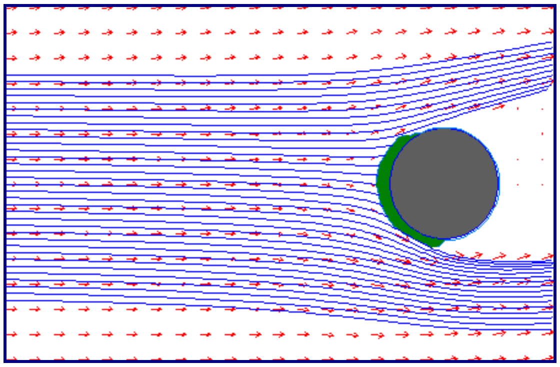

Fig 1 Airflow velocity field and trajectories of water droplets in the vicinity of an icing object
Simulation conditions: droplet diameter 26 µm, cable diameter 34.925 mm, wind speed 8m/s.

2.2 Momentum Analysis of the Water Film

In this study, the water film on an icing surface is assumed to be a steady and laminar flow which is subjected to gravity and to distributed air shear stress. Tentatively, the water film may be regarded as a flow between a fixed plate and distributed shear stress, as shown in Fig. 2. These plates are inclined at an angle θ with regard to the horizontal plane. It is possible to apply the momentum equation to an element of fluid, the top of which is the liquid surface. The element has a unit width normal to the page. The pressure is hydrostatic across any section normal to the plane, as a uniform distribution is assumed. Moreover, the depth is constant, so that the pressure forces of the end sections of the element will cancel each other out. Therefore, the momentum equation becomes:

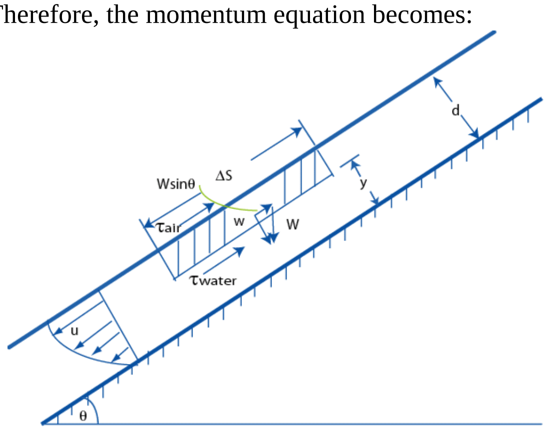

Fig. 2 Inclined flow between a fixed plate and moving plate

$$\tau \Delta s + \tau_{air} \Delta s - W \sin\theta = 0 \qquad (1)$$

Here, it is possible to substitute $\mu \frac{du}{dy}$ for τ since the thin water film under discussion may be treated as a laminar flow. The resulting differential equation may then be solved by direct integration for the velocity distribution. In order to evaluate the constant of integration, we make use of the fact that u=0 when y=0, which yields the following velocity distribution:

$$u = -\gamma(y - 2d)y \sin\theta / (2\mu) - \tau_{air} y / \mu \qquad (2)$$

The discharge per unit width is now obtained by integrating the velocity, *u*, over the depth of the flow.

$$q = \int_0^d u dy = \frac{1}{3}\frac{\gamma}{\mu} d^3 \sin\theta - \frac{\tau_{air}}{\mu}\frac{d^2}{2} \qquad (3)$$

The average velocity is given by dividing the above equation by the cross-sectional area *d*.

$$v = \frac{q}{d} = \frac{1}{3}\frac{\gamma}{\mu} d^2 \sin\theta - \frac{\tau_{air}}{\mu}\frac{d}{2} \qquad (4)$$

where the term, $\frac{1}{3}\frac{\gamma}{\mu} d^2 \sin\theta$ represents the average flow velocity induced by gravity, while $\frac{\tau_{air}}{\mu}\frac{d}{2}$ represents the velocity induced by air drag.

2.2.1 Starting Point of the Water Flow

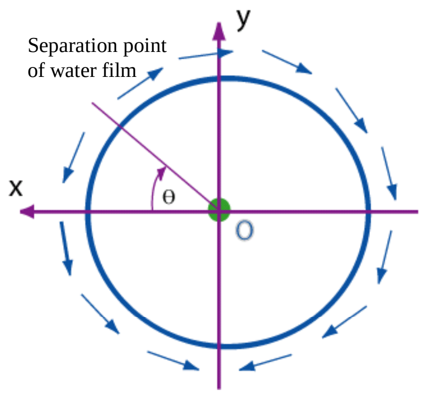

Fig. 3 Diagram for water-flow direction

On the upper half of the cylinder facing to the airflow, air shear may be dominant over gravity, which means that the water film may move upwards against the effect of gravity. As a result, two water streams may be simultaneously present on the icing surface, as indicated in Fig. 3. Accordingly, two calculation loops, corresponding to these two streams, must be performed for mass conservation and thermal balance equations in the icing code, both starting from the separation point but proceeding in opposite directions, sector by sector. Water film thickness on any given element is determined by solving the momentum equation for that particular water film. The water flow direction may eventually be determined by comparing the average flow velocities induced by gravity V_g and air drag force V_t. If V_t - V_g>0, then the water film moves upwards; otherwise, it flows downwards.

2.2.3 Conservation of mass

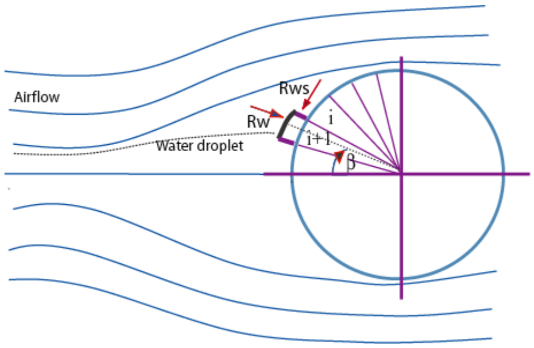

Fig. 4 Mass conservation of a water film

For any specific element, water is collected from water impingement, R_w, and unfrozen water, R_{ws}, from the preceding element, as shown in Fig. 4 where the water film is observed to move from i to $i+1$. Of the collected water, a portion, $\dot{M}_f$, will freeze while the remainder, $q\frac{\gamma}{g}$, will shift to the adjacent element. Formulating these terms in the equation of conservation of mass gives:

$$q\frac{\gamma}{g} = R_w + R_{ws} - \dot{M}_f \qquad (5)$$

where $\dot{M}_f$ represents the part of water solidified due to freezing, and it may be determined by the thermodynamics analysis provided in the next section; R_w ,which represents the part of water collected due to the airborne water flux, may be obtained from the computation of droplet trajectories; R_{ws} is the water coming from its adjacent element, derived from the calculation of its adjacent element; finally, $q\frac{\gamma}{g}$ represents the water discharge flowing to its adjacent element.

2.3 Heat Transfer in the water film

The model computes the thermodynamic conditions and the icing rate as a function of the angle around the icing cylinder.

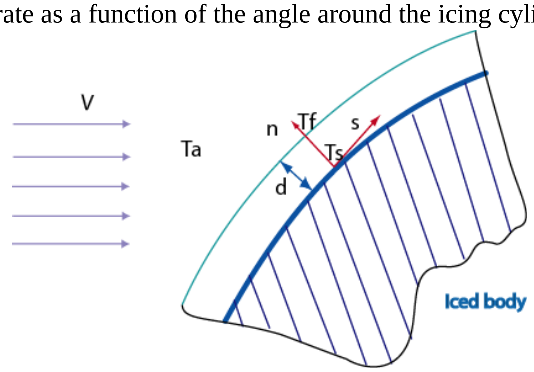

Fig. 5 Thermal balance analysis of the water film

Since temperature variations in the tangent direction and the liquid velocity component normal to the icing interface may both be neglected for a thin water film as shown in Fig. 5, the energy differential equation of the boundary layer could be written as:

$$\frac{\partial^2 T}{\partial n^2} = 0(n) \qquad (6)$$

A solution to the above equation yields a linear temperature distribution in the water film in the direction normal to icing interface.

At the air-water interface, $n=0$,

$T=T_f$, where T_f is the freezing point of the water.

At the ice-water interface, $n=d$,

$T=T_s$, where T_s is the surface temperature of the water film, initially an unknown parameter.

At the air-water interface, the heat transfer may be governed by the following equation:

$$E_{a-w} = Q_k + Q_v - Q_c - Q_e - Q_w \qquad (7)$$

where:

Q_c is the convective heat flux between the water film and the airflow streams $= -h(T_s - T_a)$,

Q_e is the evaporative heat flux $= h\left(\frac{Pr}{S_c}\right)^{0.63} \frac{\varepsilon l_v}{pc_p}(e(T_a) - e(T_s))$,

Q_v is the heat flux due to aerodynamic heating $= hr_v V^2/(2c_p)$, where V is local air speed, and r_v is the local recovery coefficient,

Q_k is the heat flux due to the conversion of droplet kinetic energy into heat $= R_w V^2/2$, where V is the droplet impact speed, and R_w the water collected locally = $W\beta V$,

Q_w is the sensible heat flux serving for the warming of the directly impinging water $= c_w R_w (T_a - T_s)$.

It should be noted that the above equation is a function of surface temperature.

At the ice-water interface, when the heat conduction through ice mass is ignored, the heat generated due to phase change may be expressed as:

$$E_{w-i} = M_f l_f \qquad (8)$$

For a linear temperature distribution, the heat flux passing through the water film should satisfy the following equation:

$$E = E_{a-w} = E_{w-i} = k_l \frac{T_s - T_f}{d} \qquad (9)$$

where d is the thickness of the water film.

2.4 Solution

Combining Eq. 3 and Eq. 5, we have:

$$\dot{M}_{in} + \dot{M}_{cl} - \frac{E}{l_\beta} = \left(\frac{1}{3}\frac{\gamma}{\mu} d^3 \sin\theta - \frac{\tau_{air}}{\mu}\frac{d^2}{2}\right)\frac{\gamma}{g} \qquad (10)$$

If, in Eq. 10, E and d are substituted by Eq. 7 and Eq. 9 respectively, the former yields the surface temperature, T_s.

Subsequently, the water-film thickness, d, may be determined by solving Eq. 9, where E is evaluated according to Eq. 7.

Lastly, the water-film velocity is obtained by solving Eq. 4.

3. Model Simulations and Validation

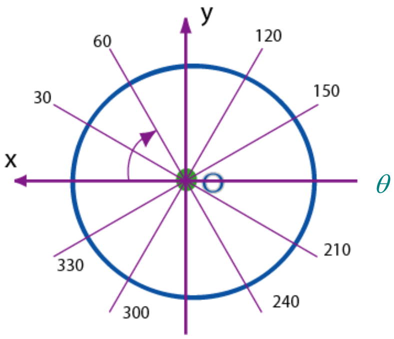

Fig. 6 Definition of angular position on cylinder surface.

In order to estimate the effects of the surface water film on the icing process, simulations were carried out for three cases, as shown in Tab. 1. Case 1 has a wind speed of 15 m/s while Case 2 and Case 3 share wind speeds of 30 m/s. LWCs in Case 2 and Case 3 are 0.375 g/m^3, only a quarter of the Case 1 value. The difference between Case 2 and Case 3 is air temperature, i.e. –5ºC for Case 2 and -7ºC for Case 3. The cylinder under consideration in all three cases is of 34.9 mm in diameter. The definition of the angular position on the cylinder is shown in Fig. 6. The simulation results for water-film thickness, surface temperature and icing fraction on the upstream side were obtained and illustrated in Fig. 7, Fig. 8, and Fig. 9, respectively.

Case No.	Model Input Parameters				
	Air Speed (m/s)	Temperature (°C)	MVD (μm)	Diameter (mm)	LWC (g/m^3)
1	15	-5	22	34.9	1.5
2	30	-5	22	34.9	0.375
3	30	-7	22	34.9	0.375

Tab. 1 Parameters used for model calculations

The curves for water-film thickness in Fig. 7 display the same trend, i.e. the water-film thickness decreases from an upper to a lower position on the upstream side of the cylinder, reaching to its minimum at the lower half of the cylinder. Such a variation is due to the fact that the water flow at a higher position moves at a lower speed, and as a result, more water accumulates at such positions. At the lower half , though, Case 1 speed shows a heavier water film because of the lower wind speed.

Figure 8 shows the distributions of the surface temperature calculated using the traditional and the new method separately, the curve in solid line representing results obtained from the new method while the curve in broken line demonstrating results from the classical method. It may be observed that the predicted temperature in the new method varies gradually over the surface, attaining to its minimum value, –1.5ºC, somewhere at the upper half of the cylinder. These results, however, undermine the traditional method which postulates that the water film maintains at a constant freezing-point temperature, as shown by the curve in broken line. It should be noted that the principal cooling heat fluxes are almost proportional to the temperature difference between air and the water surface. For fixed air temperature, the temperature difference depends solely on the surface temperature, i.e. the higher the surface temperature, the greater the temperature difference will be. The traditional method yields a higher surface temperature and thus a greater temperature difference which may further contribute to an overestimation of the icing fraction.

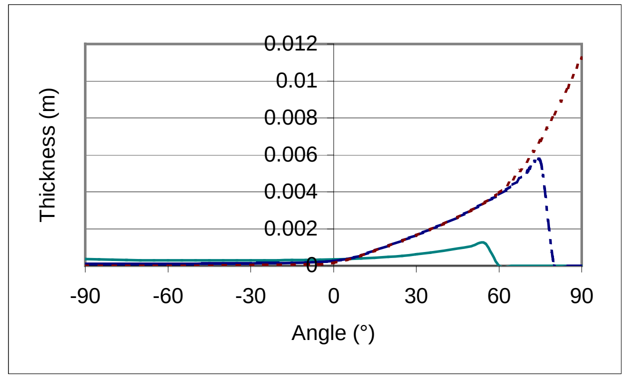

Air Speed 15 m/s, Temp. -5°C, LWC 1.5 g/m^3.
Air Speed 30 m/s, Temp. -5°C, LWC 0.375 g/m^3.
Air Speed 30 m/s, Temp. -7°C, LWC 0.375 g/m^3.

Fig. 7 Distribution of water-film thickness on the upstream side

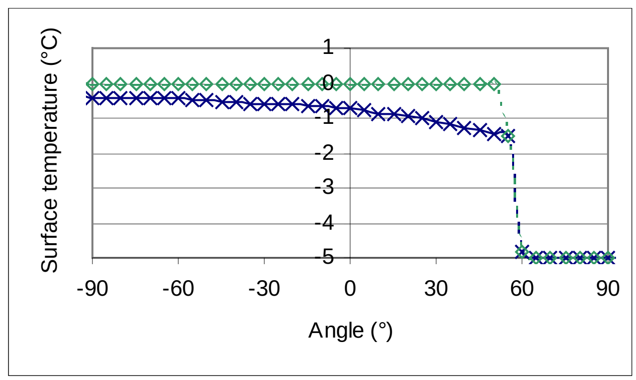

Effect of water film considered
Effect of water film not considered

Fig. 8 Distribution of water surface temperature on the upstream side
Conditions: Air Speed 15 m/s, Temperature -5°C, LWC 1.5 g/m^3 μm.

Figure 9 (a) , (b) and (c) show icing fraction distributions yet again for the three cases described earlier. Each of them shows two curves, of which the curve in solid line represents the simulation using the new method while the curve in broken line represents the one using the old method. The icing-fraction curves from both methods do show a perceivable discrepancy, especially at positions where surface temperatures differ to a great degree from the freezing point. It may also be observed in Fig. 9 that, for the case of a higher wind speed, the water-film starting point (i.e. the point of singularity) becomes even closer to the stagnation line. Moreover, the icing fraction predicted by the traditional method deviates more from the one obtained from the new method, especially at the upper half of the upstream side, where abundant water is found. Despite of these difference, the two methods produces no noticeable effects on the estimation of the icing fraction at the lower half of the cylinder, since the water film thickness at such positions is at a negligible level.

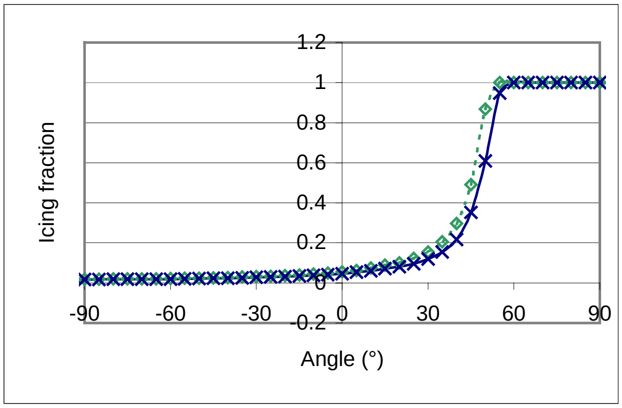

(a) Air Speed 15 m/s, Temperature -5°C, LWC 1.5 g/m^3

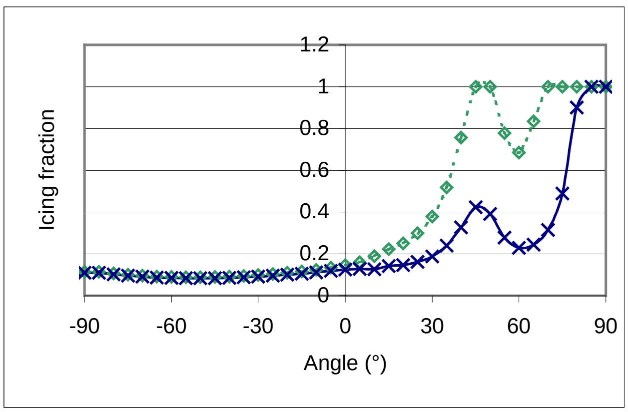

(b) Air Speed 30 m/s, Temperature -5°C, LWC 0.375 g/m^3

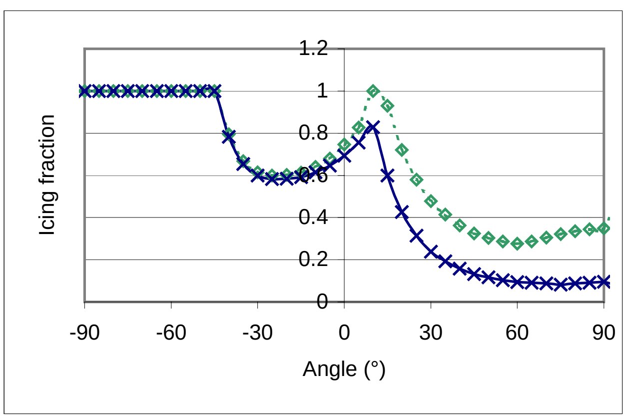

(c) Air Speed 30 m/s, Temperature -7°C, LWC 0.375 g/m^3

Effect of water film considered

Effect of water film not considered

Fig. 9 Distribution of icing fraction on the upstream side

Fig. 10 shows the shapes predicted by the ice model with the new method under the specified conditions. The shape on the right side is obtained at a higher wind speed, whereas ice mass may even be found on the leeward side of the cylinder. Under high wind conditions, part of the unfrozen water will flow in a clockwise direction, pushing its own pathway even further back. Then, under adverse cooling conditions, this water will freeze somewhere on its way downwards on the cylinder rear side.

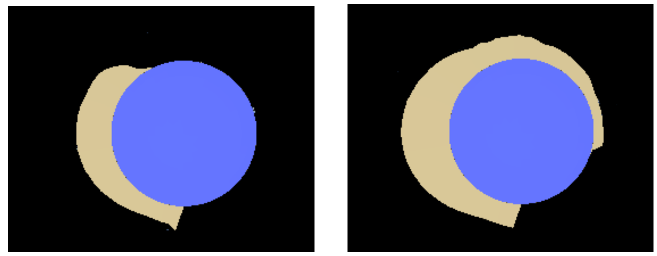

(a) **(b)**

Fig. 10 Ice shapes obtained under different icing conditions.
(a) Air Speed 10 m/s, Temp. -5°C, LWC 2.5 g/m^3 µm, MVD 26 µm.
(b) Air Speed 20 m/s, Temp. -5°C, LWC 2.5 g/m^3 µm, MVD 26 µm.

4. CONCLUSIONS

In this paper, a description of the method used to determine the local heat transfer coefficient was provided. The new method was used to investigate a number of cases, thus making possible an analysis of the momentum and thermodynamic behaviors of the water film on an icing surface. Based on this study, a number of conclusions may be drawn:

1. The water film has a major influence on the thermodynamic behavior of an icing surface. The decrease in the icing fraction resulting from the inclusion of the water film may be as high as 40% at certain positions on the upper half of the cylinder, though no perceivable change may be found at the lower half where water-film thickness is comparably insignificant.
2. The new method predicts that the surface temperature on an icing surface, in wet regime, is below the freezing point, and that the lowest temperature is found somewhere on the upper half of the cylinder, as was demonstrated experimentally [13].
3. Water film thickness on the upper half of the cylinder increases considerable so much so that the film should no longer be viewed as laminar flow there. Therefore, further study is needed in order to take this effect into account.
4. Performance of an icing model may further be enhanced by taking into account heat conduction in the ice mass.

ACKNOWLEDGMENTS

This research was carried out within the framework of the NSERC/Hydro-Quebec Industrial Chair on Atmospheric Icing of Power Network Equipment (CIGELE) and the Canada Research Chair on Atmospheric Icing Engineering of Power Network (INGIVRE) at the Université du Québec à Chicoutimi. The authors would like to thank Prof. Lozowski and Dr. Karev for usefull discussions, and all the sponsors of CIGELE/INGIVRE for their financial support.

REFERENCES

[1] Achenbach, E., "Heat transfer from smooth and rough surfaced circular cylinders in a cross flow", Proceedings of the 5th International Heat Transfer Conference, Tokyo, pp. 229-233, 1974.

[2] Bain, M. and Gayet, J.F., "Etude de l'accrétion de la glace atmosphérique. II: Modélisation numerique avec paramétristion de la variation de la mass spécifique du givre en fonction de la position angulaire sur un cylindre", *Journal de Recherches Atmosphériques*, 17, 299-311, 1983.

[3] Bourgault, Y., Beaugendre, H., Habashi, W.G., "Development of a shallow-water icing model in FENSAP-ICE", *Journal of Aircraft*, pp. 640-646, Vol. 37(4), 2000.

[4] Chen, Y., Farzaneh, M., Lozowski, E.P., and Szilder, K., "Modeling of Ice Accretion on Transmission Line Conductors", Proceedings of the 9th International Workshop on Atmospheric Icing of Structures, Chester, United Kingdom, June 2000, Session 7a.

[5] Fulford, G.D., "The flow of liquids in the thin films", *Adv. Chem. Engrg*. 5, 151-236. 1964.

[6] Fu, P., Bouchard, G., and Farzaneh, M., "Simulation of Ice Accumulation on Transmission Line Cables Based on Time-Dependent Airflow and Water Droplet Trajectory Calculations", Proceedings of the 23rd International Conference on Offshore Mechanics and Arctic Engineering, Vancouver, Canada, 2004.

[7] Gent, R.W., "TRAJICE2 - A Combined Water Droplet Trajectory and Ice Accretion Prediction Program for Aerofoil", DRA Technical Report TR90054, Nov. 1990.

[8] Gent, R.W., Dart, N.P., Cansdale, J.T., "Aircraft icing", *Philos. Trans. R. Soc*. Lond. A 358 (1776) 2873-2911, 2000.

[9] Habashi, W.G., "Putting Computers on Ice", *ICAO Journal*, Vol. 50, No. 7, pp. 14-17, October 1995.

[10] Hedde, T., "Modélisation tridimensionnelle des dépôts de givre sur les voilures d'aéronefs," Thèse/doctorat, Université Blaise Pascal, Clermont-Ferrand II, France, No. D.U. 462, Dec. 1992.

[11] Hess, J.L., and Smith, A.M.O., "Calculation of Potential Flow About Arbitrary Bodies," *Progress in Aeronautics Sciences*, Vol. 8, pp. 1-138, 1967.

[12] Hess, J.L., Review of integral-equation techniques for solving potential flow problems with emphasis on the surface-source method, *Computer Methods in Applied Mechanics and Engineering*, 5, 145, 1975.

[13] Karev, A.R., Farzaneh, M., "Infrared Laboratory Measurement of Iced Surface Temperatures during Experimental Studies on the Formation of Ice Accretions", Proceedings of The Thirteenth ISOPE, Honolulu, Hawaii, USA, May 25-30, 2003.

[14] Karev, A., Farzaneh, M., Lozowski, E.P., " Character and Stability of a Wind-Driven Supercooled Water Film on an Icing Surface, Part I : Laminar Heat Transfer ". *International Journal of Thermal Science*, Vol. 42, No. 5, mai 2003, pp. 481-498.

[15] Langmuir, I. P. and Blodgett, K. B., "Mathematical Investigation of Water Droplet Trajectories", *Program Press*, 196, Vol. 10, Report No. RL-224, 1945.

[16] Lozowski, E. P. et al. , "The icing of an unheated, non-rotating cylinder in liquid Water droplet-ice crystal clouds", National Research Council of Canada Report LTR-LT-96, 61 pp., 1979.

[17] Lozowski, E. P., Stallabrass, J. R., and Hearty, P. F., "The Icing of an Unheated, Non-rotating Cylinder, Part I: A Simulation Model", *Journal of Climate and Applied Meteorology*, Vol. 22, pp. 2053-2062, 1983.

[18] Macklin W.C., "The density and structure of ice formed by accretion," *Quarterly Journal of the Royal Meteorological Society*, pp. 30-50, 1962.

[19] McComber, P. and Bouchard, G., "The Numerical Calculation of the Wind Force Coefficients on Two Dimensional Iced Structures", Proceedings of the 3rd International Workshop on Atmospheric Icing of Structures, May 1986.

[20] Makkonen, L., " Heat transfer and icing of a rough cylinder", *Cold Regions Science and Technology*, Vol. 10, pp. 105-116, 1984.

[21] Makkonen, L., "Models for the growth of rime, glaze, icicles and wet snow on structures", *Philosophical transactions: mathematical, physical & engineering sciences*, 2000.

[22] Messinger, B. L., "Equilibrium temperature of an unheated icing surface as a function of airspeed", *Journal of the Aeronautical Sciences*, Vol. 20, pp. 195- 200, 1953.

[23] Mulherin, N. D., "Atmospheric Icing and Tower Collapse in the United States", Proceedings of the 7th International Workshop on Atmospheric Icing of Structures, June 1996.

[24] Myers, T.G., Charpin, J.P.F., "A mathematical model for atmospheric icing accretion and water flow on a old surface", *International Journal of Heat and Mass Transfer*, 5483-5500, 2004.

[25] Paraschivoiu, I., Tran, P., and Brahimi, M.T., "Prediction of Ice Accretion with Viscous Effects on Aircraft Wings," *AIAA Journal of Aircraft*, Vol. 31, No. 4, pp. 855-861, July-Aug. 1994, (also AIAA Paper 93-0027).

[26] Poots, G., "Ice and Snow Accretion on Structures," Research Studies Press LTD, 1996.

[27] Szilder, K., Farzaneh, M., and Lozowski, EP., "Analysis of Water Film Flow on an Icing Surface", Proceedings of the 9th International Workshop on Atmospheric Icing of Structures, Chester, United Kingdom, June 2000, session 4b.